Force mapping on a partially H-covered Si(111)-(7×7) surface: Influence of tip and surface reactivity

Ayhan Yurtsever,[1,2,*] Yoshiaki Sugimoto,[1] Hideki Tanaka,[1] Masayuki Abe,[1,3] Seizo Morita,[1,2] Martin Ondráček,[4] Pablo Pou,[5] Rubén Pérez,[5,6] and Pavel Jelínek[4,†]

[1]*Graduate School of Engineering, Osaka University, 2-1 Yamada Oka, Suita, Osaka 565-0871, Japan*
[2]*The Institute of Scientific and Industrial Research, Osaka University, 8-1 Mihogaoka, Ibaraki, Osaka 567-0047, Japan*
[3]*Graduate School of Engineering, Nagoya University, Furo-cho, Chikusa-ku, Nagoya 464-8603, Japan*
[4]*Institute of Physics, Academy of Sciences of the Czech Republic, Cukrovarnická 10/112, Prague 162 00, Czech Republic*
[5]*Departamento de Física Teórica de la Materia Condensada, Universidad Autónoma de Madrid, 28049 Madrid, Spain*
[6]*Condensed Matter Physics Center (IFIMAC), Universidad Autónoma de Madrid, 28049 Madrid, Spain*

(Received 14 September 2012; revised manuscript received 24 January 2013; published 4 April 2013)

We report force mapping experiments on Si(111)-(7×7) surfaces with adsorbed hydrogen, using atomic force microscopy at room temperature supported by density functional theory (DFT) simulations. On the basis of noncontact atomic force microscopy (NC-AFM) images as well as force versus distance curves measured over both hydrogen-passivated and bare Si adatoms, we identified two types of tip termination, which result in different modes of interaction with the surface. The statistics of the tip dependence of the measured forces, which are effectuated using various tip states with different cantilevers, reveal the typical values of the force and their distribution in the two characteristic interaction modes. The experimental results are corroborated by DFT calculations performed for different tip structures. As a reactive tip, the dimer-terminated Si tip yields results in satisfactory agreement with experimental force curves for hydrogen-passivated and nonpassivated Si adatom sites. An oxidized Si dimer tip that bears a hydroxyl group on its apex reproduces well the experimental force curves acquired by nonreactive tips. This tip model could thus be used to interpret the experimentally obtained weak image contrast for the Si(111)-(7×7) surface. The forces are thought to arise as a result of a weak electrostatic interaction involving a permanent dipole at the tip apex enhanced by the charge density redistribution due to the interaction with surface adatoms.

DOI: 10.1103/PhysRevB.87.155403 PACS number(s): 68.47.Fg, 68.37.Ps, 71.15.Mb, 68.43.−h

I. INTRODUCTION

Noncontact atomic force microscopy (NC-AFM) has proven to be an inestimable tool for quantifying the various kinds of interaction forces acting between an atomically sharp AFM tip and surfaces exhibiting insulating or conducting properties.[1–3] These achievements have given us the opportunity to grasp the mechanisms responsible for image contrast formation over various kinds of materials and to understand the fundamental chemical interactions that occur between the AFM tip and sample surfaces. Tremendous progress has been made in recent years in understanding the mechanisms and interactions that enable atomic-scale contrast by combining experiments with sophisticated theoretical calculations of short-range forces involved in the AFM imaging procedure.[1,3] The short-range interaction force can be determined by force spectroscopy (FS), in which forces are measured as a function of distance. In particular, FS measurements have been performed on a variety of surfaces, including semiconductors,[4,5] metals,[6,7] metal-oxides,[8] ionic crystals,[9,10] single-walled carbon nanotubes (SWNT),[11] and graphite (0001).[12] Recently, the capability of atomic-scale imaging and spectroscopic probing of interaction forces was extended to organic molecules by using a CO-functionalized metallic tip,[13] and the observed contrast was assigned to Pauli repulsion. Furthermore, the forces arising between two chemically inert CO molecules were measured.[14] The directional dependence of chemical bonding forces between a metallic tip with different crystallographic orientations and a CO molecule was investigated by three-dimensional force spectroscopy.[7] More recently, the role of tip termination and its reactivity in quantitative AFM imaging of the graphene surface were demonstrated with chemically inert (CO-terminated) and reactive tips.[15]

The above-mentioned studies clearly demonstrate the importance of the structure and chemical reactivity of the tip in NC-AFM image formation, as well as in probing the interatomic and/or intermolecular interactions. Thus a detailed understanding of the interatomic or intermolecular interactions between the two interacting elements, i.e., the surface and the front atom of a tip, requires insight into the role of the tip apex chemical reactivity. The effect of tip chemical reactivity on atomic-scale contrast has been discussed in detail on the basis of density functional theory (DFT) calculations of carbon-based materials[16] and metal-oxide surfaces.[8]

On covalent surfaces such as Si(111)-(7×7), atomic-scale contrast is primarily due to the onset of covalent bonding interaction.[17] However, it has been shown that the reactivity of the tip apex termination plays a crucial role in the image contrast constitution. Depending on the tip apex reactivity, two distinctly different types of atomic contrast can be produced on Si(111)-(7×7).[18,19] The underlying imaging mechanism of the observed weak image contrasts, as also shown in Fig. 1(b), was linked to a weak electrostatic interaction in Ref. 18 and to the van der Waals interaction in Ref. 19. Oxide-covered Si tips were proposed to explain the images of Si(111)-(7×7) exhibiting such weak corrugation. The influence of the tip chemical reactivity in the particular case of the semiconductor Si(100) surface was recently studied by Sharp

et al.[20] Furthermore, Jarvis *et al.*[21] investigated the role of the orbital alignment between the tip and hydrogen-passivated Si(100) surface in the atom manipulation process based on the atomic exchange mechanism.

In the present study, we investigate the interaction forces acting between an AFM probe and specific sites of the Si(111)-(7×7) surface exposed to a low coverage of atomic hydrogen at room temperature. We mainly focus on two issues: (i) clarifying the primary mechanisms of the interaction leading to a weak image contrast as reported for the Si(111)-(7×7) surface, and (ii) determining the characteristics of forces produced with tips varying in chemical reactivity.

The low-coverage adsorption of H atoms on Si(111)-(7×7) leads to a significant change in the chemical and electronic properties of the surface through passivation of the surface dangling bonds without surface reconstruction, which in turn can change the charge distributions.[22] By choosing a Si(111)-(7×7) surface with a small amount of adsorbed hydrogen for our study, we ensure that our model surface involves reactive as well as chemically inert, nonreactive sites. At the same time, both reactive and nonreactive tips can be expected to appear in the AFM on this surface, just as in the case of a clean Si(111)-(7×7) surface. Thus the partially H-passivated Si(111)-(7×7) allows us to characterize the interaction between the surface sites and the tip for all four possible combinations: reactive or nonreactive sites with a reactive or nonreactive tip.

A previous investigation has shown that the measured force exhibits some variability depending on the chemical and structural properties of the tip apex.[5,8,23–26] In order to obtain reliable information regarding the ranges and relative strengths of the forces associated with the different interaction modes, it is essential to perform the force measurements with a large number of tips. In contrast to a well-defined tip, with an unknown tip apex termination, it is indispensable to take into account the tip dependence of the measured forces. In other words, a large number of data sets is required for a correct understanding of the role played by the tip chemical reactivity in probing the different interaction forces and their distribution.

Systematic two-dimensional force mapping measurements performed with different cantilevers and tip terminations allowed us to quantify the strength and distance dependence of forces in the different characteristic regimes. Our experimental results were corroborated by DFT calculations performed for different atomic models of tips in order to interpret the observed force curves, particularly the ones that contribute to the weaker type of image contrast on the Si(111)-(7×7) surface. Projected density of states (PDOS) calculations combined with charge density difference maps provide an explanation for the mechanisms of interaction forces observed in experiments on the H: Si(111)-(7×7) surface.

II. EXPERIMENTAL PROCEDURES

Experiments were carried out using a custom-built ultrahigh-vacuum NC-AFM operated at room temperature (RT) with a base pressure better than 6×10^{-9} Pa. The NC-AFM was operated using a frequency modulation detection mode,[27] keeping the cantilever oscillation amplitude constant. We used commercial silicon cantilevers (Nanosensor NCLR), which were cleaned by Ar ion sputtering to remove the native oxide layer and contaminants. The clean Si(111)-(7×7) reconstructed surfaces were prepared by the standard method, i.e., flashing the sample up to 1200 °C for a few seconds and reducing the temperature to about 900 °C, and then slowly decreasing to RT. Molecular hydrogen (H_2) was first introduced into the preparation chamber through a leak valve. Then, the H_2 molecule was dissociated into atomic hydrogen by heating a tungsten filament, located 10 cm from the surface. After the surface was cooled to RT, it was exposed to H atoms under a pressure of 9.3×10^{-7} Pa for 30 s. The sample was then transferred into an observation chamber housing the NC-AFM for investigation. The bias voltage (Vs) applied to the sample surface, with the tip held at ground potential, was adjusted to minimize the long-range electrostatic forces. Precise tip positioning and thermal drift compensation during force mapping is achieved by using atom tracking and feed-forward software.[28,29] Two-dimensional (2D) force mapping was performed, recording the induced frequency shift (Δf) from the resonance frequency by constant height scanning while gradually increasing the tip-sample distance (z). For further details on the force mapping procedure, we refer the reader to Ref. 30.

III. COMPUTATIONAL PROCEDURES

Our DFT calculations presented here have been performed using the VASP code,[31] employing ultrasoft plane-wave pseudopotentials[32,33] and the generalized-gradient approximation (GGA) with the PW91 functional[34] as the exchange-correlation energy. We use a plane-wave cutoff energy of 200 eV. The H/Si(111)-(7×7) surface structure has been modeled by periodically repeated seven-layer Si slabs separated by a vacuum gap of 15 Å [see Fig. 5(a)]. The dangling bonds on atoms in the base of the tips and in the bottom of the surface slab were saturated by hydrogen atoms. All atomic positions in both the slab and the tip, except for the bottommost Si layer, the base atomic layer of the tip, and the saturating hydrogen atoms attached to these Si layers, were allowed to relax freely at every step of the simulated tip approach until the energy and forces converged to 10^{-6} eV and 0.05 eV/Å, respectively. Two types of tip model structures were used in our theoretical calculations of the tip-surface interaction. We have modeled the tips by silicon-based clusters built upon either (111) or (001) surface orientations. The tip derived from the (111)-oriented surface consisted of a ten-atom Si cluster with a single dangling bond sticking out of the apex. This tip model has been used previously in Ref. 17, reproducing well the short-range chemical force on Si adatom sites.[4] The other class of tip models was derived from a larger Si cluster grown in the (001) direction and terminated with a Si dimer (i.e., dimer tip). In addition to the Si-dimer-terminated tip itself, other tips within this class had their apices modified by the adsorption of a hydrogen atom, oxygen atom, or an OH functional group. The details and the basic criteria applied for the selection of model tips are described in Ref. 35. See inset of Fig. 5 for ball-and-stick models of the tips.

The GGA form of the exchange-correlation functional does not account for nonlocal effects such as the interaction of dynamically-induced dipoles, the so-called London dispersion

forces. However, this kind of interaction mainly creates a long-range background, which is rather featureless at the atomic scale.[13,16] We subtract this background from our experimental data in the way described below. Thus the omission of the London dispersion forces does not preclude a comparison between the calculated and measured forces.

IV. RESULTS AND DISCUSSION

A. NC-AFM imaging of H atoms on Si(111)-(7×7)

Mainly two types of topographic images have been identified for Si(111)-(7×7) by NC-AFM, depending on the tip apex reactivity, as previously observed for the bare Si(111)-(7×7) surface.[18,19] These two types of contrast mode, acquired with two different types of tip termination, are presented in Figs. 1(a) and 1(b). Figure 1(a) shows an NC-AFM image of the H-adsorbed Si(111)-(7×7) surface, which was recorded with a typical reactive tip. The image in Fig. 1(b), which shows a relatively faint contrast as compared to Fig. 1(a), was acquired using the same cantilever as Fig. 1(a), but it was obtained using a typical nonreactive tip. The dark atomic features located on the Si adatom sites in Figs. 1(a) and 1(b) are assigned to hydrogen-passivated adatoms. To confirm that these are H atoms appearing dark in the images, the hydrogen atom exposure time was varied during the experiment. It was clearly observed that the number of dark sites increases with exposure time. The adsorbed H atoms in these images appear as dark depressions, implying a rather weak attractive interaction above the H-passivated Si adatoms as compared with the clean Si adatom sites. The hydrogen adsorption and its energetics on the Si(111)-(7×7) surface has been extensively studied before, both experimentally and theoretically, in Refs. 36–38. It has been demonstrated that the H atoms preferentially reside on the rest atom sites. However, the diffusion energy barrier between Si adatoms and rest atom sites is too large to be overcome by hydrogen atoms so that some of the H atoms can also occupy the less favorable Si adatom sites at RT. Unlike the scanning tunneling microscopy (STM) image of the surface showing the hydrogen atoms residing on both the Si adatom and rest atom sites, the NC-AFM images shown here only resolve the H atoms that are located on top of the Si adatom sites. The invisibility of the hydrogen atoms on rest atom sites by NC-AFM imaging was confirmed by simultaneous STM/AFM images. The STM images showed signs indicating the adsorption of H atoms over the rest atom sites (not shown here). However, the focus of the present investigations is to study atomic tip-sample interactions from the perspective of tip and surface reactivity.

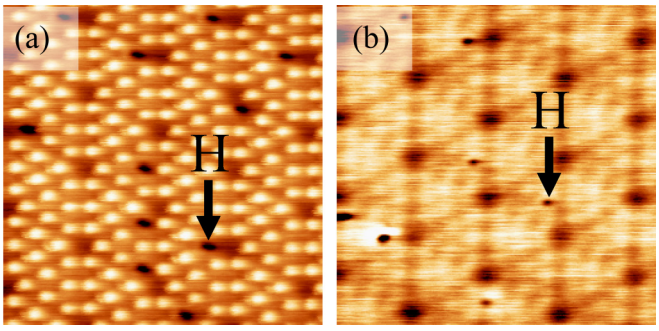

FIG. 1. (Color online) NC-AFM topographic images of the Si(111)-(7×7) surface exposed to a low-coverage of H atoms at room temperature, recorded with (a) a reactive and (b) a nonreactive tips. Note that hydrogen adsorbed on an adatom appears as a depression in both images (see text). NC-AFM resolves only the H atoms that reside on Si adatom sites. The arrows mark the H adatoms. The acquisition parameters were (a) $f_0 = 172.577$ kHz, $k = 41.1$ N/m, $A = 16.4$ nm, $\Delta f = -8.3$ Hz, and $Vs = -250$ mV; (b) $A = 22.5$ nm, $\Delta f = -7.2$ Hz, and $Vs = -200$ mV. The same cantilever was used for both images. The image size is 10×10 nm^2, in both (a) and (b) .

B. Force mapping

In order to get more insight into the nature of the interaction between the Si surface with adsorbed atomic hydrogen and the different tips that leads to the characteristic images shown in Figs. 1(a) and 1(b), two-dimensional (2D) Δf mapping was performed along the path traversing the long diagonal of the 7×7 unit cell of the Si(111)-(7×7) surface (see Fig. 2). In Figs. 2(a) and 2(c), we show the resulting raw data image of the Δf maps of the H-adsorbed Si(111)-(7×7) surfaces, which were acquired with a reactive and a chemically inert nonreactive tip, respectively. After subtraction of the long-range force contribution, which was measured above the corner hole site, the resulting short-range Δf maps were converted into short-range force (F_{SR}) maps using the well established conversion formula, as described in Ref. 39. The fluctuations of Δf observed in Figs. 2(a) and 3(a) for small z in the curve acquired at the H-passivated site (see especially the insets of the figures) prevented us from converting Δf into force in the corresponding distance range. The solid white rectangle shown in Fig. 2(b) indicates the excluded data points in the force map.

The typical F_{SR} maps of a surface exposed to H atoms, acquired with a reactive tip and a nonreactive tip, are displayed in Figs. 2(b) and 2(d), respectively. Although the hydrogen atoms on the Si(111)-(7×7) surface were identified directly in the NC-AFM images (see section A), the hydrogen-passivated Si adatoms are also clearly distinguishable from the clean Si adatoms in the force maps. The clean Si adatoms have a stronger attraction to the tips. The force map acquired by a reactive tip reveals only a single H adatom, whereas the force map recorded by a nonreactive tip indicates five different H atoms located on Si adatom sites. Although the numbers of H atoms exposed are identical in both images shown in Fig. 1, we coincidentally selected a path having a large number of H atoms in the force mapping experiment acquired by a nonreactive tip.

In Figs. 3(a) and 3(c), we show the distance dependence of the $\Delta f(z)$ curves extracted from the 2D Δf maps shown in Figs. 2(a) and 2(c), respectively. The corresponding individual F_{SR} curves above the selected sites (marked with dashed lines in Fig. 2) are displayed in Figs. 3(b) and 3(d), respectively. For a reactive tip, the force data indicate a small attractive interaction on H-passivated Si adatoms, while a strong attractive force acts on the tip over bare Si adatom sites. The attraction between the reactive tip and Si adatoms can be ascribed to the onset of covalent bonding between

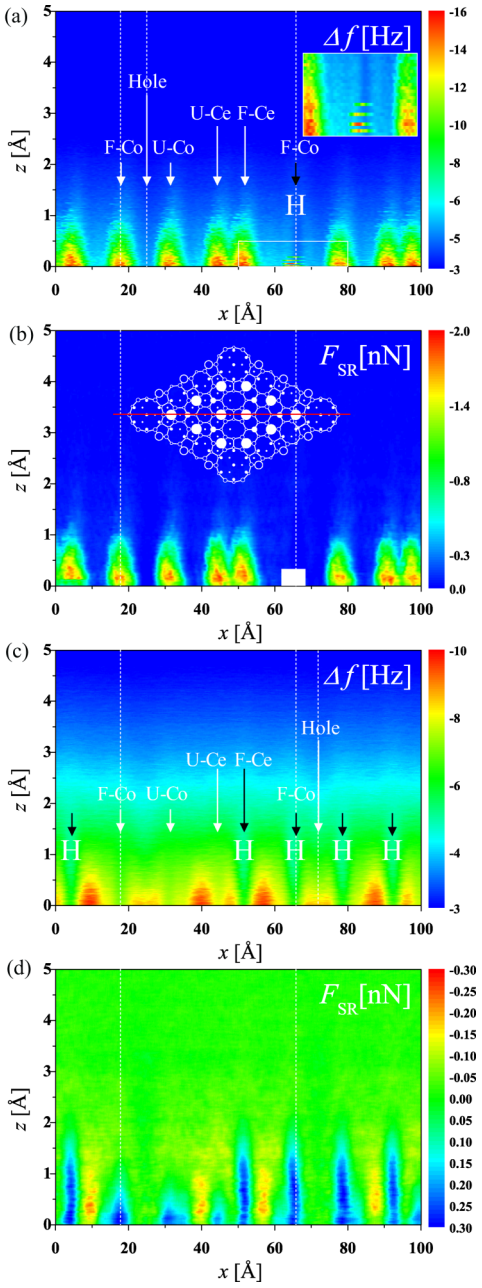

FIG. 2. (Color online) Two-dimensional Δf maps along the path traversing the long diagonal of the 7×7 unit cell acquired with (a) a reactive and (c) a nonreactive tips over the partly hydrogenated Si(111)-(7×7) surface. (b) and (d) are the short-range force maps converted from (a) and (c), respectively. The origin of the z axis is defined as the minimum distance between the tip and surface during data acquisition. The white arrows indicate faulted corner (F-Co), faulted center (F-Ce), unfaulted corner (U-Co), unfaulted center (U-Ce), and corner hole (Hole) sites. The hydrogen-passivated Si atoms are indicated by black arrows. The inset of (a) contains a zoom of the H-passivated site. The DAS model for the Si(111)-(7×7) surface was depicted in the inset of (b) to assign the features of the 7×7 structure. The white dashed lines indicate the positions where we extracted the spectroscopic curves shown in Fig. 3. The color-coded map scale is indicated on the right side of each image. The acquisition parameters were (a) $f_0 = 169.913$ kHz, $k = 38.7$ N/m, $A = 20.7$ nm, and $Vs = -250$ mV; (b) $f_0 = 172.577$ kHz, $k = 41.1$ N/m, $A = 21.9$ nm, and $Vs = -200$ mV.

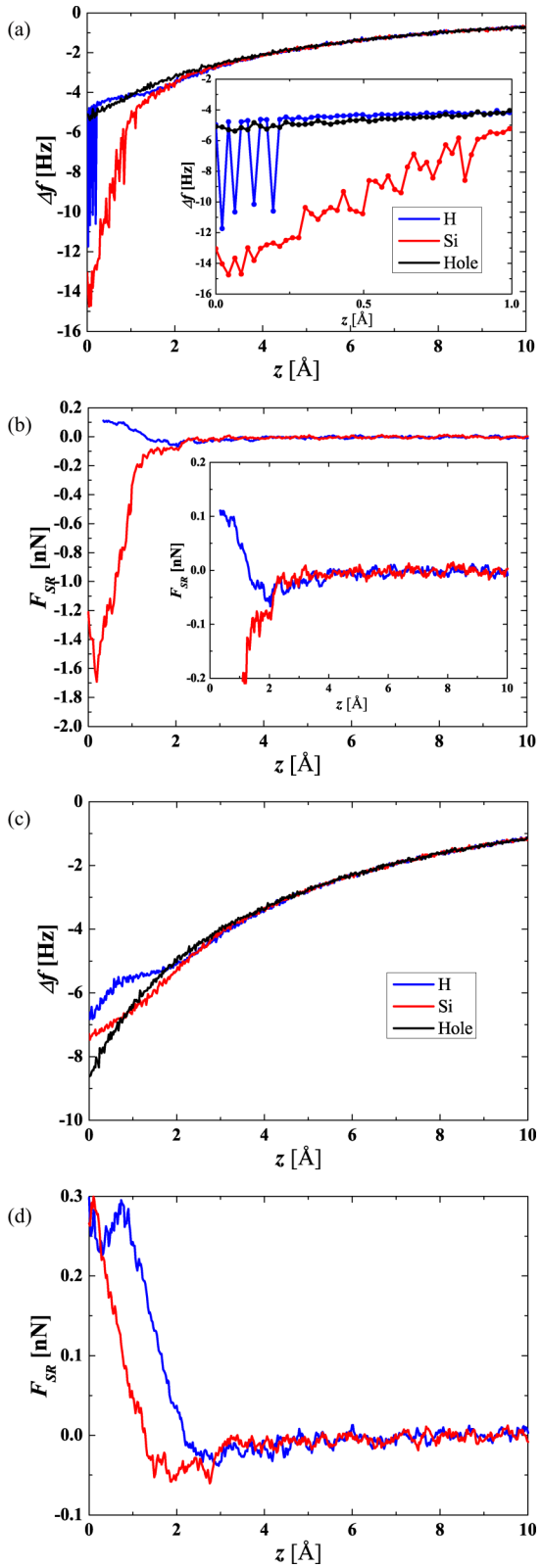

FIG. 3. (Color online) Individual Δf curves extracted from 2D Δf maps measured above a Si adatom (red), hydrogen-passivated Si adatom (blue), and corner hole (black), recorded with (a) a reactive and (c) a nonreactive tips. The region of small tip-sample distance is highlighted in the inset of (a). (b) and (d) Short-range interaction force (F_{SR}) curves derived from (a) and (c), respectively. The inset of (b) shows the short-range forces plotted on an expanded scale.

the dangling bonds on the Si adatoms and the tip apex atom (cf. Ref. 17). By contrast, with a nonreactive tip, force spectroscopy data both on H-passivated Si and clean Si adatom sites show a small attractive force with a magnitude below 0.1 nN.

At a smaller tip-sample separation, we see an increasing repulsive force that can be ascribed to the Pauli repulsion. The repulsion first arises above the H-passivated Si adatoms for reactive as well as nonreactive tips, as the tip-sample separation is gradually decreased. With the nonreactive tips, the repulsion is also achieved on bare Si adatoms if the tip approaches yet closer, by about 1 Å with respect to the distance where the repulsion starts on the H-passivated adatoms. In addition, at close tip-sample distances, a decrease in the repulsive branch of the force curve over the hydrogen atom site was observed [see Figs. 3(d)]. We may attribute this behavior to the relaxation at the tip or surface atom positions, caused by the tip-surface interactions. At close tip-sample distances, the tip apex or surface atoms undergo relaxation, the tip apex atom and the surface H atom start to repel each other, and one of these atoms bends sideways. This rearrangement of hydrogen atom positions leads to an additional attractive interaction with neighboring Si adatoms. The resulting attractive interaction reduces the repulsive force between the tip apex atom and the surface hydrogen atom. Thus a slight decrease in the repulsive force occurs at such close distances. More interestingly, below a certain tip-sample distance, the force curve for the H-passivated adatom follows the same behavior as the curve for the Si adatom. This suggests that the observed relaxation was completed and thus the tip-surface interaction became similar for both atomic sites.

The above mentioned fluctuations, which are apparent in the frequency shift versus distance curve shown in the inset of Fig. 3(a), suggest the presence of a bistability that shows up as a transition from a stronger to a weaker interacting state and vice versa. This transition is clearly associated with the existence of two metastable configurations of the tip-surface system having nearly the same energies.[40,41] However, we can only speculate as to the actual structural difference between these two states. It may, for example, be related to the reconfiguration of the Si-bonded H atom: the Si-H bond tends to bend as the repulsive force from the tip pushes the H atom away, possibly resulting in two metastable configurations distinguished by the angle between the Si-H bond and the surface. Despite the observed jumps in the frequency shift curves at small distances, the simultaneously recorded dissipation mapping exhibits no distinct signal on these sites within the limit of experimental noise. However, it was demonstrated that the dissipation arising from the atomic instabilities has a strong temperature dependence, and can be smoothed out by increasing the temperature.[40] Therefore we believe that the inaccessibility of the dissipation signal might be caused by a temperature effect.

To investigate the tip dependence of the magnitude of the measured force maxima, we have carried out the same experiment using eight cantilevers with 30 different tip states exhibiting both reactive and inert (nonreactive) properties. The statistics of these measurements are summarized in Figs. 4(a) and 4(b). If we characterize the tip-adatom interaction by the maximal value of the attractive short-range force, we obtain

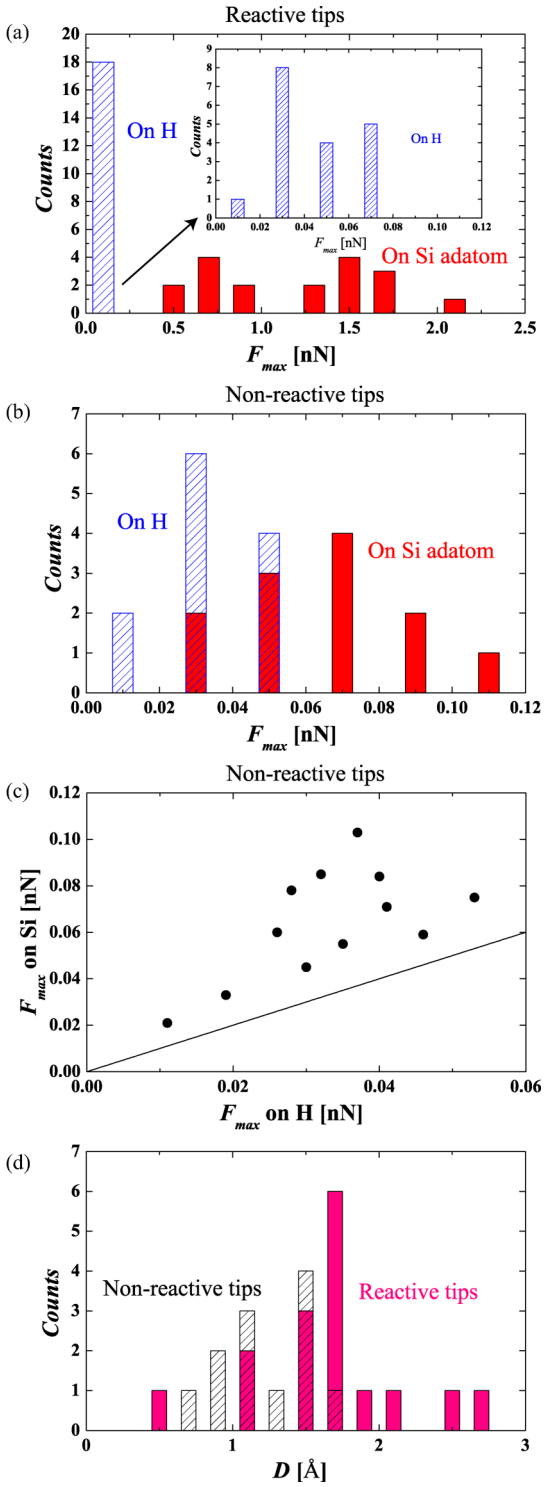

FIG. 4. (Color online) Histograms of the maximum attractive short-range force (F_{SR}) above Si and H-passivated Si adatoms obtained with (a) reactive and (b) nonreactive tips, produced by using 30 different tips with eight cantilevers. Details of the histograms obtained for hydrogen-passivated Si adatoms is indicated in the inset of (a). (c) Correlation of the maximum attractive short-range force (F_{SR}) above Si and H-passivated Si adatoms obtained with nonreactive tips [see (b)]. The solid line shows the direct proportionality between the force maxima for clarity. (d) Histogram of the difference of distances of maximum attractive F_{SR} between Si and H-passivated Si adatoms.

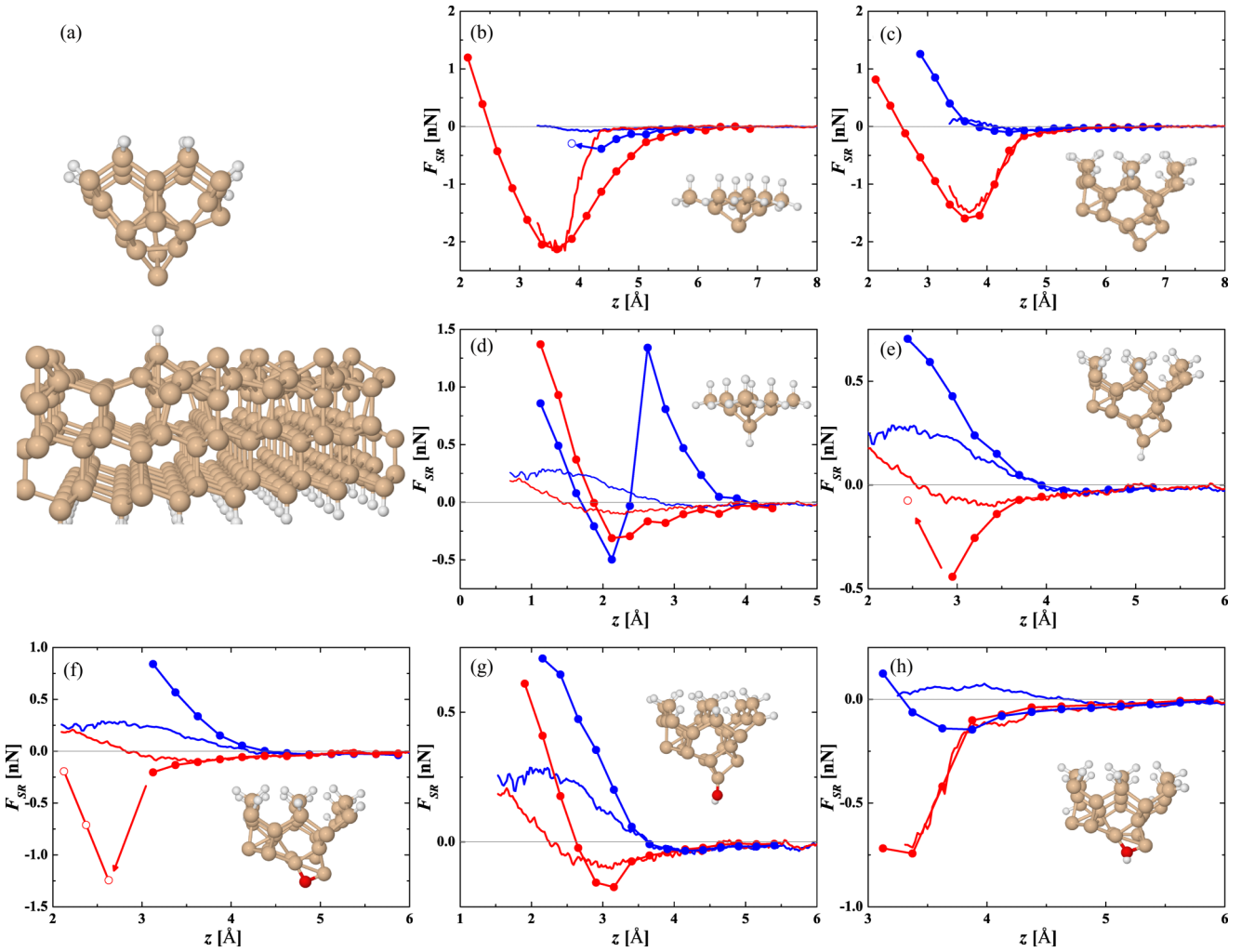

FIG. 5. (Color online) (a) Schematic of the tip and H-adsorbed Si surface used in our simulation. Calculated short-range interaction forces over Si (red line with circles) and hydrogen-passivated Si (blue line with circles) adatoms for various tip models: (b) an H3-Si(111), (c) Si(001) dimer, (d) hydrogen-terminated H3-Si, (e) hydrogen-terminated Si dimer, (f) double-bonded O-terminated Si dimer, (g) OH-terminated Si dimer, and (h) double-bonded OH-terminated Si dimer tips. The color code for the ball-and-stick models is as follows: red corresponds to O, white to H, and cream to Si. Selected experimental force curves (continuous lines) are included for comparison: experimental curves that fit best the theoretical prediction with respect to the maximal attractive force were selected for each panel, i.e., for each tip model.

two well-separated interaction modes that correspond to two distinct ranges of the characteristic short-range forces.

With reactive tips, the average maximum attractive force above H-terminated Si adatoms was 0.042 nN, whereas the distribution of the forces above unsaturated Si adatom sites exhibits a broad spectrum varying from 0.56 to 2.15 nN. The presence of such a broad distribution of attractive force maxima reveals the varying degree of reactivity found within the class of reactive tips. Nevertheless, a clear distinction is observed between the forces over reactive and H-passivated nonreactive adatom sites [see Fig. 4(a)]. In the case of nonreactive tips, a smaller difference with an average value of 0.03 nN was found in the maximal force between the two distinct adatom sites [see Fig. 4(b)]. The respective ranges of the maximal attractive force observed on the H-passivated and bare Si adatom sites with various noninteracting tips even overlap, as seen in Fig. 4(b). For any given nonreactive tip, however, the maximal attractive force on the H-passivated site is still always smaller than on a clean Si adatom [see Fig. 4(c)]. Moreover, the two kinds of surface sites can also be distinguished on the basis of the tip-surface distance at which the maximal attractive force occurs. The histogram of distance differences between force maxima for the two sites is plotted in Fig. 4(d) for both reactive and nonreactive tips.

The comparison of the force distribution obtained using a reactive tip with the nonreactive H-passivated surface site on the one hand, and a nonreactive tip with the reactive Si adatom site on the other, can elucidate the relationship between the structure and reactivity of the tip (for the importance of this relationship, see also, e.g., Refs. 5 and 42). Evidently, the interaction between a reactive tip and a nonreactive site results in a force distribution similar to that between a nonreactive tip and a reactive site, both leading to a maximum attractive force of around 0.05 nN. This observation suggests that the

formation of a nonreactive tip involves the adsorption of a hydrogen atom on the tip. Specific models of nonreactive tips will be discussed in the following section.

To sum up, from the characteristics of the observed image contrast as well as the force spectra measured on the reactive and nonreactive surface sites, we have found that AFM tips can be classified into two main groups, one characterized by reactive behavior, the other by nonreactive behavior.

C. Identification of tip structure using DFT

In order to be able to interpret the experimental evidence, we carry out a series of DFT calculations, using several tip models with different chemical activities. Our aim is to identify plausible tip models that can explain the most common types of NC-AFM images and force curves encountered in the experiment. Once we have suitable candidates to describe the tip structure, we can further use first-principles calculations to determine the mechanism of interaction between these tips and the surface. The tip structures represented by our models were made of Si clusters grown in the (001) and (111) surface orientations. The apices of the tips may or may not be contaminated by singly and/or doubly bonded oxygen or hydrogen atoms or a hydroxyl group (for the tip models, see insets of Fig. 5). As our simulations show, the contamination typically reduces the strength of interaction between the tip and the surface. Our calculation results are summarized in Fig. 5, which plots the calculated short-range forces as a function of distance for a tip over Si and H-terminated Si adatoms. For comparison, we include in each panel of Fig. 5 a typical experimental curve obtained either with a reactive tip (in the case of Si-only tip models) or a nonreactive tip (in the case of contaminated tip models). Figures 6(a) and 6(b) show in greater detail the results for the two most successful tip models along with the corresponding experimental curves.

Figure 6(a) plots the short-range forces obtained with the dimer-terminated Si tip. The Si dimer tip correctly reproduces the experimentally obtained maximal attractive forces on the relevant surface sites. The maximum force calculated for this particular tip is about 1.6 nN for Si and 0.1 nN for H-passivated Si adatom sites, which is in good agreement with the experimental results [see, for example, Fig. 3(b)] in the case of reactive tips. However, the location of the attractive force maxima, i.e., the tip height difference between the respective maxima on the bare Si and on the H-passivated adatom, does not fit the experimental curves so well. The distribution of the distances between the maximum attractive forces above the specified sites is shown in Fig. 4(d), which reveals an average difference of 1.6 Å with a reactive tip (and of 1.2 Å with a nonreactive tip). Furthermore, the stiffness of the force curve on the hydrogen-terminated Si adatom does not match the experimental curves. These discrepancies can be attributed to the extent of relaxation of tip apex atoms treated by the simulation. The elastic properties of a realistic tip apex cannot be accurately reproduced within the limited size of models used for the tip in our calculations. The effect of the force field experienced by the tip should ideally be transferred over a large part of the apex cluster, thus reducing the strain field by distributing it across the many atoms. In the absence of this property, an overestimation of stiffness occurs, which becomes apparent especially in the curves at small distances corresponding to the repulsive regime. A similar effect of limited tip cluster size on AFM simulations was found in Ref. 8. However, such discrepancy is acceptable for quantitative evaluation of the tip-surface interactions in the region of strongest attraction, where it is presumably less significant than in the repulsive regime. Another pure Si tip model, the Si(111) tip with its apex atom in the H3 position [force curves shown in Fig. 5(a)], turns out to be unstable, because it tends to collect hydrogen atoms from the surface. This model is therefore not a suitable candidate to represent the reactive tips encountered in the present experiment. Let us note that an analogous transfer of hydrogen atom was predicted in Ref. 21 for AFM on the Si(100) surface.

The spread of values found for the maximal attractive force in the case of reactive tips [see Fig. 4(a)] indicates that there was a large diversity of apex structures among the reactive tips in our experiment. The proposed model of the dimer-terminated Si tip is just a representative example of possible

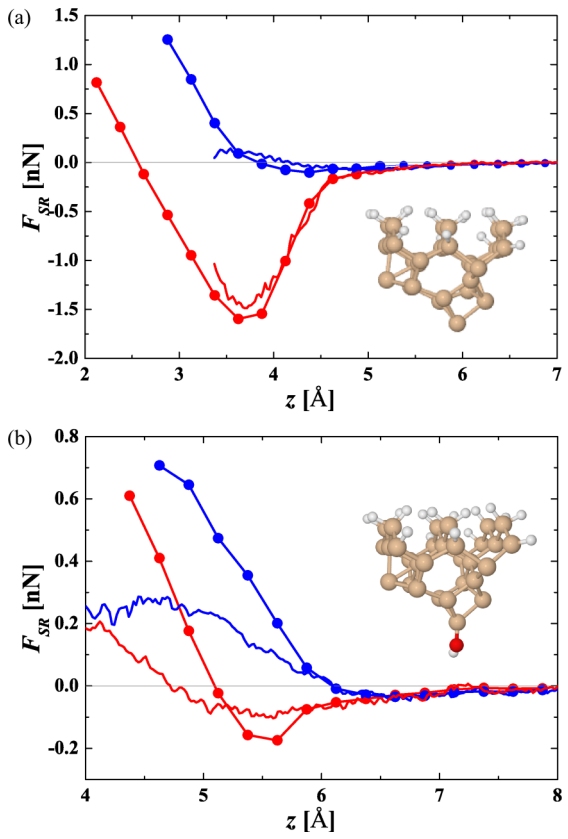

FIG. 6. (Color online) Measured (continuous curves) and calculated (circles connected with lines) short-range interaction force over Si (red) and hydrogen-passivated Si (blue) adatoms obtained with (a) a Si (001) dimer tip, and (b) an OH-terminated Si dimer tip. The experimental curves shown here have been chosen out of those obtained with (a) a strongly interacting and (b) a nonreactive tips. To compare with theoretical curves, the experimental force curves have been shifted to superpose the force minima over Si adatoms with respect to Fig. 3. The acquisition parameters were (a) $f_0 = 169.920$ kHz, $k = 38.7$ N/m, $A = 27.5$ nm, and $Vs = -200$ mV; (b) $f_0 = 172.577$ kHz, $k = 41.1$ N/m, $A = 21.9$ nm, and $Vs = -200$ mV.

tip structures in the class of reactive tips, not one which would explain every single reactive tip. See Ref. 35 as an example of diversity within a group of similar Si tips.

For the purpose of simulating nonreactive tips, the model shown in the insets of Figs. 5(g) and 6(b) proves the most promising. This model was created from a Si(001) cluster terminated with an OH functional group. Such a tip may form in an experimental situation where a partially oxidized Si tip picks a hydrogen atom from either the surface or the residual gas inside the vacuum chamber. The hydrogen-atom termination assumed for the tip is justified by the NC-AFM images, as shown in Fig. 1(b). The image contrast shown in Fig. 1(b) was observed only rarely on bare Si(111)-(7×7), on which no H atoms were adsorbed, while the frequency of observing the same type of contrast was dramatically increased when hydrogen was allowed to adsorb on the Si(111) surface. Just like the experimental force data for nonreactive tips, the Si(001)-based OH-terminated tip exhibits the same basic trend of small attractive force on both types of atomic sites [see Fig. 6(b)]. The magnitude of the maximal attractive force predicted by this tip model over the H-terminated adatom sites agrees very well with the value measured on the H-passivated adatoms with nonreactive tips. However, the maximal force prediction for the nonpassivated (bare) Si adatom site is somewhat larger than the forces observed for these adatom sites experimentally. Moreover, we observe that the slopes of the force curves for the OH-terminated tip deviate from those of the experimentally obtained curves in the repulsive region. The overestimation of the stiffness of the force curves in the repulsive regime once again (as in the case of reactive tips) points to the increased rigidity of the spatially restricted models of tip apices considered in our simulations. The inaccurately described relaxation of the tip geometry may be also related to the overestimation of the attractive force maximum calculated on the Si adatom. The O-H bond on the tip is tilted with respect to the surface normal, and the tilting angle changes because of the interaction between the apex H atom and the nearby adatom if the tip gets close to the Si surface. The short-range force acting on the tip is sensitive to the tilting angle of the OH group because as the H atom of the group moves aside, direct interaction between the Si adatom and the oxygen atom on the tip becomes possible. While, in reality, the deformation induced in the tip by the approaching surface could be distributed over the many tip atoms, in the relatively rigid model cluster, the OH group has to accommodate most of the deformation, which leads to the observed differences between simulation and experiment.

We have also considered the possibility of a purely oxidized tip, without any hydrogen attached. However, our model for such a tip exhibits an instability as it jumps to contact as it approaches the Si adatom [see Fig. 5(f)]. Upon this jump to contact, the tip structure changes—the oxygen atom at the tip termination binds to the adatom, forming a bridge between the tip and the adatom—and the attractive force increases abruptly to about 1.2 nN, at variance with our experimental data for nonreactive tips. On the other hand, one may argue that nonreactive tips can be regarded simply as hydrogen-contaminated Si tips, without the presence of oxygen. We have indeed tried this type of tip model, too, but it turns out that these tips also tend to be unstable as they approach the Si surface. Even though the extraction of H atoms from the surface by the tip was occasionally observed over the course of the mapping experiments, we excluded such cases from the collection of experimental data used in the subsequent analysis. Only the results acquired without tip apex changes were considered suitable to characterize the forces on reactive as well as nonreactive surface sites at the same time. Therefore the stable nonreactive tips cannot be explained by the models that consist of a H apex atom on a Si cluster.

Finally, let us note that, as with the reactive tips, the OH-terminated Si dimer tip, which we propose as the preferred model of a nonreactive tip, represents a whole class of real tips which may differ in structural details. Nevertheless, on the basis of the above arguments, we believe that an OH group at the very end of the tip is a common feature of the various nonreactive tips encountered in our experiments.

D. Interaction mechanism

To obtain more specific information about the cause of the interaction force, we investigated the evolution of the projected density of states (PDOS) on the Si adatoms [see Figs. 7(b)–7(e)] and the electron density redistribution associated with the presence of the interaction with the tip [see Fig. 7(a)]. We constructed the electron density redistribution maps by determining the electron density of the interacting system of the tip and surface and subtracting from this density, first, the electron density calculated for the tip alone, and second, the electron density calculated for the surface alone. Figure 7(a) shows such maps at the maxima of the attractive interaction force for three different models of the tip placed above a Si adatom. The color code is as follows: the red end of the color spectrum corresponds to electron depletion, while the blue-violet end corresponds to electron enhancement. We see that, for all tip models, electron redistribution upon tip-adatom interaction leads to increased electron density in the space between the tip apex and adatom. The redistribution is the weakest, but still noticeable, for the tip with an OH termination bonded to a silicon dimer [the rightmost frame in Fig. 7(a)], which is also the tip that gives the lowest attractive force maximum.

Let us now look at the PDOS. Figure 7(b) shows the PDOS for the Si adatom when the tip is far away from the surface ($z = 7$ Å), which is the same as that obtained in the absence of the tip. Compare this with the PDOS for the same atom when a tip is placed at a distance where the attractive force reaches its maximum. The Si-dimer-terminated tip changes the adatom PDOS dramatically, as shown in Fig. 7(d). The complete rearrangement of PDOS peaks, which split and shift with respect to the noninteracting case, indicates that the original atomic orbitals on the adatom hybridize with those on the tip apex atom to form new bonding and antibonding orbitals, thus establishing a chemical bond. Similarly, the tip with the OH group double-bonded to the Si cluster also notably perturbs the PDOS on the Si adatom PDOS, although not as much as the Si dimer tip. Again, the changes of the PDOS indicate that hybridization occurs between the adatom and

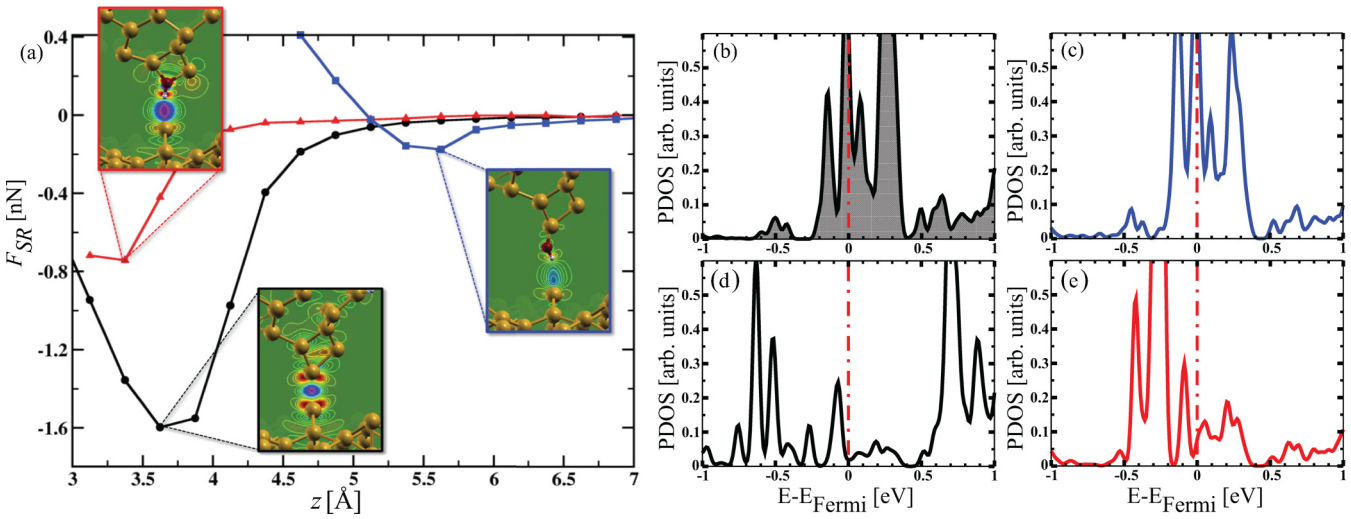

FIG. 7. (Color online) (a) Exemplary short-range force curves for three tip models on a Si adatom on the Si(111)-(7×7) surface. (Inset) The electron density difference maps between tip models and a surface Si adatom (color code: violet and blue denotes electron density enhancement, red denotes electron density depletion) at a distance close to the maximum of each particular short-range force. Calculated projected density of states (PDOS) at the distance corresponding to attractive force maxima above a Si adatom on the Si(111)-(7×7) surface, performed with (c) a Si dimer-OH, (d) a dimer, and (e) a double-bonded OH-terminated Si dimer tips. The PDOS on a Si adatom in the absence of the tip-sample interaction is shown in (b).

tip apex orbitals. This points out the presence of chemical interaction.

In contrast to the two previously discussed model tips, the weakly interacting tip with a single-bonded OH group termination hardly changes the PDOS, as seen in Fig. 7(c). The positions of the peaks remain the same, only their relative weights change a bit. This indicates that there is no formation of a chemical bond. In this particular case, the interaction between the tip and Si adatom is mainly driven by electrostatic interaction. According to our analysis of electron density distribution on the Si adatom, there is a weak dipole moment oriented with its positive pole out of the surface. This observation is in good agreement with previous experimental evidence.[43] This dipole interacts predominantly with the negatively charged OH group at the apex of the tip, resulting in a weak attractive interaction. Moreover, additional charge redistribution [see the rightmost frame in Fig. 7(a)], caused by mutual tip-sample interaction, occurs upon tip approach towards the surface. The short-range force arising with a weakly interacting tip is thus caused by complex electrostatic interaction, which involves permanent as well as induced dipoles on the tip and the surface. This type of interaction is similar to that proposed in Ref. 18 for an oxidized tip over a clean Si(111)-(7×7) surface. However, our calculations indicate that weakly reactive tips are terminated by hydroxyl group rather than a native SiO_2 oxide layer. Therefore, in contrast to the above cited work, our tip model bears not only an induced but also a permanent electric-dipole component on the apex. Furthermore, the OH group can quite easily respond to applied forces by tilting towards or away from the surface. This mobility of the H atom in the OH group also influences the tip-surface interaction, as discussed in Ref. 25.

V. CONCLUSION

We have explored the interaction between tips exhibiting either reactive or nonreactive characteristics with a hydrogen-adsorbate-covered Si(111)-(7×7) surface at RT. Our results represent a direct comparison of different interaction regimes ranging from strong (chemisorption-related) to weak (physisorption-related) interaction forces arising between the tip and surface. DFT calculations reveal the possible structures of tip apex termination that can produce the experimentally observed forces. It is found that oxidized Si dimer tips that possess a hydrogen atom at the apex (i.e., OH-terminated tips) might provide a suitable model to explain the experimentally obtained weak interatomic forces associated with a nonreactive tip on the H: Si(111)-(7×7) surface. We combined the PDOS with maps of electron density redistribution at the tip-sample interface to identify the mechanisms of the weak tip-surface interaction. We attribute this interaction to a weak electrostatic interaction between the tip termination and the surface charge associated with the Si adatoms.

ACKNOWLEDGMENTS

This work was supported by Grants-in-Aid for Scientific Research (22221006, 24360016, 24651116, and 22760028) from the Ministry of Education, Culture, Sports, Science and Technology (MEXT) of Japan, Funding Program for Next Generation World-Leading Researchers. This work is also supported by MAT2011-23627, CSD2010-00024, PLE2009-0061 (MINECO, Spain). P.P. was supported by the Ramón y Cajal program (MINECO, Spain). We further acknowledge the support provided by the Czech Science Foundation (GAČR) under the projects P204/11/P578 and P204/10/0952, the GAAV project IAA100100905 and project M100101207.

*ayhan@afm.eei.eng.osaka-u.ac.jp
†jelinekp@fzu.cz

[1]*Noncontact Atomic Force Microscopy*, edited by S. Morita, F. J. Giessibl, and R. Wiesendanger, Vol. 2 (Springer-Verlag, Berlin-Heidelberg, 2009).
[2]F. J. Giessibl, Rev. Mod. Phys. **75**, 949 (2003).
[3]R. Garcia and R. Perez, Surf. Sci. Rep. **47**, 197 (2002).
[4]M. A. Lantz, H. J. Hug, R. Hoffmann, P. J. A. van Schendel, P. Kappenberger, S. Martin, A. Baratoff, and H. J. Guntherodt, Science **291**, 2580 (2001).
[5]Y. Sugimoto, P. Pou, M. Abe, P. Jelínek, R. Pérez, S. Morita, and O. Custance, Nature (London) **446**, 64 (2007).
[6]M. Ternes, C. González, C. P. Lutz, P. Hapala, F. J. Giessibl, P. Jelínek, and A. J. Heinrich, Phys. Rev. Lett. **106**, 016802 (2011).
[7]J. Welker and F. J. Giessibl, Science **336**, 444 (2012).
[8]A. Yurtsever, D. Fernandez-Torre, C. Gonzalez, P. Jelinek, P. Pou, Y. Sugimoto, M. Abe, R. Perez, and S. Morita, Phys. Rev. B **85**, 125416 (2012).
[9]M. A. Lantz, R. Hoffmann, A. S. Foster, A. Baratoff, H. J. Hug, H. R. Hidber, and H. J. Güntherodt, Phys. Rev. B **74**, 245426 (2006).
[10]R. Hoffmann, C. Barth, A. S. Foster, A. L. Shluger, H. J. Hug, H. J. Güntherodt, R. M. Nieminen, and M. Reichling, J. Am. Chem. Soc. **127**, 17863 (2005).
[11]M. Ashino, A. Schwarz, T. Behnke, and R. Wiesendanger, Phys. Rev. Lett. **93**, 136101 (2004).
[12]H. Hölscher, W. Allers, U. D. Schwarz, A. Schwarz, and R. Wiesendanger, Phys. Rev. B **62**, 6967 (2000).
[13]L. Gross, F. Mohn, N. Moll, P. Liljeroth, and G. Meyer, Science **325**, 1110 (2009).
[14]Z. Sun, M. P. Boneschanscher, I. Swart, D. Vanmaekelbergh, and P. Liljeroth, Phys. Rev. Lett. **106**, 046104 (2011).
[15]M. P. Boneschanscher, J. van der Lit, Z. Sun, I. Swart, P. Liljeroth, and D. Vanmaekelbergh, ACS Nano **6**, 10216 (2012).
[16]M. Ondráček, P. Pou, V. Rozsíval, C. González, P. Jelínek, and R. Pérez, Phys. Rev. Lett. **106**, 176101 (2011).
[17]R. Perez, M. C. Payne, I. Stich, and K. Terakura, Phys. Rev. Lett. **78**, 678 (1997).
[18]M. A. Lantz, H. J. Hug, R. Hoffmann, S. Martin, A. Baratoff, and H. J. Güntherodt, Phys. Rev. B **68**, 035324 (2003).
[19]S. Morita, Y. Sugawara, K. Yokoyama, and T. Uchihashi, Nanotechnology **11**, 120 (2000).
[20]P. Sharp, S. Jarvis, R. Woolley, A. Sweetman, L. Kantorovich, C. Pakes, and P. Moriaty, Appl. Phys. Lett. **100**, 233120 (2012).
[21]S. Jarvis, A. Sweetman, J. Bamidele, L. Kantorovich, and P. Moriarty, Phys. Rev. B **85**, 235305 (2012).
[22]T. Klitsner and J. S. Nelson, Phys. Rev. Lett. **67**, 3800 (1991).
[23]A. S. Foster, A. Y. Gal, Y. J. Lee, A. L. Shluger, and R. M. Nieminen, Appl. Surf. Sci. **210**, 146 (2003).
[24]G. H. Enevoldsen, A. S. Foster, M. C. Christensen, J. V. Lauritsen, and F. Besenbacher, Phys. Rev. B **76**, 205415 (2007).
[25]R. Bechstein, C. González, J. Schütte, P. Jelínek, R. Perez, and A. Kühnle, Nanotechnology **20**, 505703 (2009).
[26]A. Campbellová, M. Ondráček, P. Pou, R. Pérez, P. Klapetek, and P. Jelínek, Nanotechnology **22**, 295710 (2011).
[27]T. R. Albrecht, P. Grütter, D. Horne, and D. Rugar, J. Appl. Phys. **69**, 668 (1991).
[28]M. Abe, Y. Sugimoto, O. Custance, and S. Morita, Appl. Phys. Lett. **87**, 173503 (2005).
[29]M. Abe, Y. Sugimoto, T. Namikawa, K. Morita, N. Oyabu, and S. Morita, Appl. Phys. Lett. **90**, 203103 (2007).
[30]Y. Sugimoto, T. Namikawa, K. Miki, M. Abe, and S. Morita, Phys. Rev. B **77**, 195424 (2008).
[31]G. Kresse and J. Furthmüller, Phys. Rev. B **54**, 11169 (1996).
[32]D. Vanderbilt, Phys. Rev. B **41**, 7892 (1990).
[33]G. Kresse and J. Hafner, J. Phys.: Condens. Matter **6**, 8245 (1994).
[34]J. P. Perdew, J. A. Chevary, S. H. Vosko, K. A. Jackson, M. R. Pederson, D. J. Singh, and C. Fiolhais, Phys. Rev. B **46**, 6671 (1992).
[35]P. Pou, S. A. Ghasemi, P. Jelinek, T. Lenosky, S. Goedecker, and R. Perez, Nanotechnology **20**, 264015 (2009).
[36]I. C. Razado, H. M. Zhang, R. I. G. Uhrberg, and G. V. Hansson, Phys. Rev. B **71**, 235411 (2005).
[37]R.-L. Lo, I.-S. Hwang, M.-S. Ho, and T. T. Tsong, Phys. Rev. Lett. **80**, 5584 (1998).
[38]A. Vittadini and A. Selloni, Phys. Rev. Lett. **75**, 4756 (1995).
[39]J. E. Sader and S. P. Jarvis, Appl. Phys. Lett. **84**, 1801 (2004).
[40]L. N. Kantorovich and T. Trevethan, Phys. Rev. Lett. **93**, 236102 (2004).
[41]N. Oyabu, P. Pou, Y. Sugimoto, P. Jelinek, M. Abe, S. Morita, R. Pérez, and O. Custance, Phys. Rev. Lett. **96**, 106101 (2006).
[42]M. Setvín, P. Mutombo, M. Ondráček, Z. Majzik, M. Švec, V. Cháb, I. Ošt'ádal, P. Sobotík, and P. Jelínek, ACS Nano **8**, 6969 (2012).
[43]Y. Cho and R. Hirose, Phys. Rev. Lett. **99**, 186101 (2007).